SCATTERING FROM ROUGH SURFACES

*Peter D. Thorne and **Nicholas G. Pace
* Institute of Oceanographic Sciences, Bidston Observatory, Bidston, Birkenhead, Merseyside L43 7RA, England
** School of Physics, University of Bath, Claverton Down, Bath BA2 7AY

1. INTRODUCTION

Laboratory measurements of underwater acoustic scattering from constructed rough surfaces to examine the validity of theoretical developments has been an approach frequently adopted, [1-10] due to the difficulties in obtaining accurate and reliable scattering data from known seabeds in the marine environment. A theoretical description of surface scattering which has proved useful in explaining the laboratory data has been that obtained by solving the Helmholtz integral using the Kirchhoff approximations. [11-16] In the present study this solution is applied to scattering from both a pressure release model rough surface and marine sediments. An examination of its applicability to describe accurately the frequency, range, and angular dependence of acoustic scattering from a number of surfaces is conducted.

Measurements are presented on scattering from a low density expanded polyurethane surface with Gaussian statistics over an extremely broad frequency range, between 20-1200kHz. For the surface employed this covered a roughness parameter range, g, between 0.14-490. To obtain a source with sufficient bandwidth performance and directivity the parametric array [17-21] was employed for the lower frequency measurements. A series of range dependent experiments are also presented, which were taken at 250kHz on the expanded polyurethane surface and a gravel surface with a mean particle diameter of 8.2mm. Observations were made by keeping the transducer fixed at 150cm from the surface and an on axis miniature hydrophone measured the normal incidence backscattered signal between 2-144cm. Further angular backscattered intensity measurements are analysed which were obtained using three surfaces composed of marine gravels having different mean particle diameters. The data were collected with a sidescan geometry, using a transducer which acted as source and receiver, and had a narrow horizontal beamwidth and a broad beamwidth in the azimuth direction. All the data collected for each of the series of experiments were converted to a standard scattering coefficient and comparisons made with predictions calculated using the Helmholtz-Kirchhoff integral.

2. THEORY

2.1 Solution of Helmholtz-Kirchhoff integral

The scattering coefficient S_c is defined[22] by the following equation

$$S_c = \langle I \rangle R_o^2 R_1^2 / I_o A R_{ref}^2 \tag{1}$$

where $\langle I \rangle = \langle pp^* \rangle / 2\rho c$, p is the measured pressure and p^* is its complex conjugate, ρc is the specific acoustic impedance of the fluid, R_o and R_1 are the source and receiver distances respectively, from the scattering surface, and I_o is the source intensity at the reference distance R_{ref} (=1m). A is the insonified area on the surface which is specified by the intersection of the e^{-1} contour of the combined source and receiver pressure beam patterns. To determine $\langle I \rangle$ the scattering of the incident radiation from the rough surface is evaluated using the Helmholtz integral[11]

$$p(r) = \frac{1}{4\pi} \int_S \left[p \frac{\partial}{\partial n} \frac{\exp(ikr)}{r} - \frac{\exp(ikr)}{r} \frac{\partial p}{\partial n} \right] dS \tag{2}$$

where p(r) is the pressure at distance, r, from dS, the surface element, to the observation point, n is the normal to dS drawn towards the half space containing the source and receiver, and p and $\partial p / \partial n$ are the values of the pressure and its normal derivatives on the surface. To evaluate the latter two quantities the Kirchhoff method consists of approximating these values by those that would be present on a tangental plane at this point giving

$$p = R p_i \qquad \frac{\partial p}{\partial n} = -R \frac{\partial p_i}{\partial n} \qquad , \quad R = \frac{Z_2 \mathrm{Cos}\theta_1 - Z_1 \mathrm{Cos}\theta_2}{Z_2 \mathrm{Cos}\theta_1 + Z_1 \mathrm{Cos}\theta_2} \tag{3}$$

where p_i is the incident field, and R is the plane surface reflection coefficient. The validity of the tangental plane approximation is usually formulated by an inequality of the type[23]

$$kR_c \, \mathrm{Sin}^3\psi >> 1 \tag{4}$$

where k is the scalar wave number of the insonifying radiation, R_c is the local radius of curvature, and ψ is the local grazing angle.

The solution of the Helmholtz-Kirchhoff integral has been conducted by a number of authors,[11-16] and for the present case the solution adopted[24] when evaluating the integral uses a Fresnel phase approximation, and is formulated for a surface which can be represented by Gaussian statistics, and has source and receiver beam patterns which can be described using Gaussian directivity functions. Evaluation of the Helmholtz-Kirchhoff integral under these conditions yields a value for the scattering coefficient given by[25]

$$S_c = \frac{R^2 D^2 R_o^2 R_1^2}{(R_o + R_1)^2 A} \exp(-g) + \frac{R^2 F^2 XY}{8A} \frac{T_1 T_2}{\gamma^2 h^2} M(g)$$

$$M(g) = g \exp(-g) \sum \frac{g^n}{n!} \left[\exp\left(-\frac{T_1^2 k^2 \alpha^2}{4(S_1 T_1^2 + n)}\right) \times \exp\left(-\frac{T_2^2 k^2 \beta^2}{4(S_2 T_2^2 + n)}\right) \right.$$

$$\left. \times \left[(S_1 T_1^2 + n)^{\frac{1}{2}} (S_2 T_2^2 + n)^{\frac{1}{2}} \right]^{-1} \right] \tag{5}$$

where

$$\alpha = \mathrm{Sin}\theta_1 - \mathrm{Sin}\theta_2\mathrm{Cos}\theta_3 \qquad \beta = -\mathrm{Sin}\theta_2\mathrm{Sin}\theta_3 \qquad \gamma = -(\mathrm{Cos}\theta_1 + \mathrm{Cos}\theta_2)$$

$$F = (1 + \mathrm{Cos}\theta_1\mathrm{Cos}\theta_2 - \mathrm{Sin}\theta_1\mathrm{Sin}\theta_2\mathrm{Cos}\theta_3)/(\mathrm{Cos}\theta_1 + \mathrm{Cos}\theta_2)$$

$$U_1 = \frac{1}{2}\left(\frac{\mathrm{Cos}^2\theta_1}{R_0} + \frac{1 - \mathrm{Sin}^2\theta_2\mathrm{Cos}^2\theta_3}{R_1}\right) \qquad U_2 = \frac{1}{2}\left(\frac{1}{R_0} + \frac{1 - \mathrm{Sin}^2\theta_2\mathrm{Sin}^2\theta_3}{R_1}\right)$$

$$S_1 = \frac{1}{2}\left\{(1/X^2) + X^2k^2U_1^2\right\} \qquad S_2 = \frac{1}{2}\left\{(1/Y^2) + Y^2k^2U_2^2\right\}$$

$$D = \exp\left[-(x^2/X^2 + y^2/Y^2)\right] \qquad g = (hk\gamma)^2$$

A is the insonified area, $A = \pi XY$, D is the combined source/receiver directivity function, T_1 and T_2 are orthogonal surface autocorrelation lengths, h is the surface rms height and g is the roughness parameter. As seen in fig. 1 θ_1 is the angle of incidence, θ_2 is the scattering angle (both of which are measured with respect to the surface normal), and θ_3 is the angle between the scattered and incident planes. There are two components contributing to the total scattering coefficient. These are firstly the exp(-g) term, which is the coherent component of the scattered signal, and is effectively an attenuated reflected signal, and the second term, the incoherent component, associated with scattering from the surface.

Under a number of circumstances the expression can be much simplified and these are considered. In all cases the orthogonal correlation lengths are treated as equal $T_1 = T_2$ and the incident and scattered signals are assumed to be in the same plane, $\theta_3 = 0$.

2.2 Farfield specular direction

In this case $\alpha = \beta = 0$, F=1 and S_1 and S_2 become negligible, this now gives

$$S_c = \frac{R^2R_0^2R_1^2}{\pi(R_0+R_1)^2XY}\exp(-g) + \frac{R^2}{4\pi\sigma^2\gamma^2}\left[g\exp(-g)\sum\frac{g^n}{nn!}\right] \qquad (6)$$

where σ is the surface rms slope, $\sigma = 2h^2/T^2$. For high frequencies g>10 then $\exp(-g) \sim 0$, $M(g) \sim 1$, and at normal incidence, $\gamma = 2$, this further reduces to

$$S_c = R^2/16\pi\sigma^2 \qquad (7)$$

which is an extremely simple expression with the scattering coefficient being a function of surface slope and reflection coefficient.

2.3 High frequency solution in specular direction

In this case $\alpha = \beta = 0$, $e^{-g} \sim 0$, and we have the approximation

$$M(g) \sim ((S_1T^2/g)+1)^{-\frac{1}{2}}\ ((S_2T^2/g)+1)^{-\frac{1}{2}} \qquad (8)$$

we now have

$$S_c = \frac{R^2}{4\pi\sigma^2\gamma^2}\left[((S_1T^2/g)+1)((S_2T^2/g)+1)\right]^{-\frac{1}{2}} \qquad (9)$$

For normal incidence backscattering with an axisymetric source and receiver X=Y, and with the acknowledgement that the approximation

$$S_1 = S_2 \sim \frac{X^2k^2}{8}\left(\frac{1}{R_0} + \frac{1}{R_1}\right)^2$$

may always be made then

$$S_c = \frac{R^2}{16\pi\sigma^2}\left[1 + \frac{\Theta_0}{16\sigma^2}\left(1 + \frac{R_0}{R_1}\right)^2\right]^{-1} \qquad (10)$$

where $\Theta_o = X/R_o$. Equation 10 gives the high frequency range dependence of the scattering coefficient. In the farfield, $R_o/R_1 << (4\sigma/\Theta_o)-1$, the expression reduces to equation 7. Close to the surface, $R_o/R_1 >> (4\sigma/\Theta_o)-1$,

$$S_c = \frac{R^2}{A}\left(\frac{R_1R_0}{R_0+R_1}\right)^2 \qquad (11)$$

This is interestingly the solution for a plane surface, and therefore at high frequencies close to the surface there is no information on the surface statistics.

2.4 Farfield Backscattering

For the case when $\Theta_2 = -\Theta_1$ and $S_1=S_2\sim 0$ the scattering coefficient becomes

$$S_c = \frac{R^2}{16\pi\sigma^2\mathrm{Cos}^4\Theta_1}\, g\exp(-g)\sum \frac{g}{nn!}\exp[-g(\mathrm{Tan}^2\Theta_1/2\sigma^2 n)] \qquad (12)$$

This is valid off normal incidence when the coherent component will be negligible for a direction source. At high frequencies g>10 this reduces to

$$S_c = \frac{R^2}{16\pi\sigma^2\mathrm{Cos}^4\Theta_1}\exp[-g(\mathrm{Tan}^2\Theta_1/2\sigma^2)] \qquad (13)$$

For $\Theta_1=0$ this reduces to equation 7.

The expressions developed in this section are compared below with measured scattering coefficients from surfaces represented by Gaussian statistics, and an examination of the limitations of the Helmholtz-Kirchhoff integral approach are discussed.

3. SURFACES EMPLOYED

3.1 Expanded polyurethane surfaces

A generally accepted prerequisite for applying the Helmholtz-Kirchhoff integral is that the surface should consist of irregularities with radii of curvature much larger than the wavelength of insonification. The surface was therefore required to be gently undulating in form, having large radii of curvature over its area, and for consistancy with the theoretical approach to have a relief which could be represented by Gaussian statistics. A low impedance polyurethane surface was constructed to fulfill these requirements. Surface parameters were h=2.2m, $T(T_1=T_2)$=19mm, and R=0.93. Fig 2 shows the surface to be well represented using a Gaussian description.

3.2 Sediment surfaces

Three surfaces composed of marine sediments having mean particle diameters of 5.2, 8.5, and 24mm were employed. In fig 3 are shown the results of measurements of the surface statistics and comparisons made with a Gaussian description. The height distributions and the surface autocorrelation functions are moderately well modelled using a Gaussian representation, although the measured height distribution is negatively skewed. Details of the surfaces were; A) h=1.1mm, T=2.2mm; B) h=1.8mm, T=3.3mm; and C) h=4.1mm, T=8mm. Surface reflection coefficient measurements gave R=0.6 $\pm$ 0.2.

4. MEASUREMENTS AND ANALYSIS

4.1 Broadband results

A series of underwater acoustic normal incident ensemble average backscatter measurements were taken between 20-1200kHz on the expanded polyurethane surface. To obtain such a broad frequency of operation using one simply designed transducer advantage was taken of quarterwave plate matching layers, and the unique directional and bandwidth properties of the parametric array. Measurements between 600-1200kHz were taken using a 2.5cm diameter 1MHZ resonance PZT ceramic disc broadbanded using a quarterwave matching layer. Using the same transducer to radiate the primary frequencies a parametric source was generated using the non-linearity of the medium, and measurements taken using the difference frequency component between 20-300kHz. This frequency range available allowed an examination of the scattered signal from almost totally coherent scattering, reflection, through to the regime of large random phase variations within a scattering region giving incoherent scattering.

The results of the measurements are shown in fig 4. The scattering coefficient can be seen to be relatively constant in value over the full frequency span. A comparison of the Helmholtz-Kirchhoff predictions using equation 5 is shown by the hatched area. The predicted values are in excellent agreement over the whole frequency range with the data. Below 30HKz the coherent component dominates and effectively reflection is occurring. Above 120kHz the incoherent component is predominant and beyond 200kHz the scattering coefficient is constant and given by equation 7. These results and others[25] show the validity of the Helmholtz-Kirchhoff integral approach for near normal incident backscattering calculations from a smoothly undulating surface.

4.2 Range dependence scattering

Following on from the broadband study the normal incident range dependence of the average backscattering coefficient was investigated.[26] Measurements were carried out at 250kHz, with the transducer at 150cm from the rough surface, and the receiver range varying between 2-144cm. The results are shown in fig 5 where measurements are presented of scattering from the expanded polyurethane surface and gravel surface (B). The measurements show a rapid increase in scattering coefficient close to the surface, with a reduction in gradient on moving outwards from the surface, and finally attaining a relatively constant value. Comparison of the high frequency solution of equation 5 given in equation 10 is compared with data. It can be seen that there is good agreement over the full range of distances covered. Near to the surface, S_{NF} given by equation 11, compares well with the data and the surface responds as though it were plane. In the

farfield of the surface, S_{FF} calculated from equation 7, agrees well with the data. These measurements show that the Fresnel solution of the Helmholtz-Kirchhoff integral is quite capable of predicting the range dependence scattering coefficient, from an isotropic rough surface, to within a distance only a few times larger than the surface mean peak to trough height.

4.3 Angular backscattering

A series of measurements of the angular dependence of the backscattering coefficient from marine sediments was also conducted. The three gravel surfaces described in section 3 were employed, and measurements were taken between 10°-60° grazing angle. The observations were taken using a 300kHz transducer having a -3dB full beamwidth of 25° and 3° respectively for the vertical and horizontal direciton. The 300kHz transducer, which acted as source and receiver, was placed at a 100cm from the surface, and the ensemble average backscattered intensity was obtained by averaging over a number of swaths the time series envelope of the returned signal amplitude squared as the pulse propagated along the surface. The results of the measurements are shown in fig 6, where it can be seen that over the region where data was taken, there is a relatively steady reduction of the scattering coefficient as the grazing angle, θ_g ($=90-\theta_i$), reduced. For surface (B) measurements were also taken at 250kHz and 1MHz near normal incidence, and these have values similar to those obtained at 40°. The hatched area shown in the figures was computed using equation 12, with one standard deviation in R, σ, and θ accounted for. In general for the three figures there is good agreement with the experimental data although there is a tendency to underestimate the scattering coefficient. In fig 6 for surface (A) predictions are valid down to 10° grazing angle, while for surface (B) between 15°-90° the results compare well with the data. However, for surface (C) there is some discrepancy below 25°, unfortunately no measurements were taken below 20° for comparison with the theory.

5. DISCUSSION AND CONCLUSION

A large number of measurements under well defined conditions on scattering from a number of rough surfaces have been presented and compared with the Helmholtz-Kirchhoff integral solution for rough surface scattering.

The limitations generally placed upon the validity of the Kirchhoff solution are determined by the adequacy with which the wave is reflected at each surface point as if from a tangent plane at that point, together with the effect of neglecting any surface shadowing or multiple scattering. It has been estimated[23] that the tangent plane approximation is valid when the inequality given in (4) is valid. Local parameters are difficult to specify experimentally therefore using average terms we have $\psi \sim \theta_g$ and it has been shown[25] that $R_c \sim T^2/2\sqrt{2}h$. For the normal incidence frequency and range dependence measurements there is no shadowing or multiple scattering and therefore the only condition for validity is $kR_c >> 1$. For the expanded polyurethane surface $\bar{R}_c$=6cm and for gravel surface (B) $\bar{R}_c$=0.2cm. At the lowest frequency employed, 20kHz, for the data given in fig 4 $k\bar{R}_c$=5. Therefore all the conditions are fulfilled for a valid solution for the Helmholtz-Kirchhoff integral, and as shown there is excellent agreement with the measurements. For the range dependence observations $k\bar{R}_c$ = 63 and $k\bar{R}_c$=2 for the expanded polyurethane and the gravel surfaces respectively. In the case of the expanded polyurethane surface the

inequality of (4) is well met while for gravel surface (B) the inequality only just holds, however, in both cases theoretical agreement with data is good, although in the farfield the predictions are better for the polyurethane case. For the backscattering measurement in fig 6 $kR_c Sin^3\theta_g \leq 1$ for surfaces(A) and (B). However, even though there is some underestimate in the predictions, the Helmholtz-Kirchhoff solution gives results very similar to those measured and therefore suggest that inequality (4) may be over restrictive. Other recent work on sinusoidal surfaces[27] has also indicated that an equality such as that given in (4) may not be a reliable guide to limitations of the Kirchhoff approximation.

In summary the Helmholtz-Kirchhoff integral solution has been shown to be in good agreement with data over a broad frequency span, for ranges very close and distant from the surface, and over a large range of backscattering angles even when inequality (4) is not adhered to.

REFERENCES

1. J. M. Proud, R. T. Beyer and P. Tamarkin. Reflection of sound from randomly rough surfaces. J. of Applied Physics Vol 31 (3) 543-552 (1960)

2. G. R. Banard, C. W. Horton, M. K. Miller. Underwater-sound reflection from a pressure-release sinuisoidal surface. J. Acoust Soc Am Vol 39 (6) 1162-1169 (1966).

3. C. W. Horton, S. K. Mitchell, and G. R. Barnard. Model studies of the scattering of acoustic waves from a rough surface. J. Acoust Soc Am Vol 41 (3= 635-643 (1967).

4. P. J. Welton, H. G. Frey and P. Moore. Experimental measurements of the scattering of acoustic waves by rough services. J. Acoust Soc Am Vol 52 (5 pt 2) 1553-1563.

5. H. Medwin, J. Baillie, J. Bremhorst, B. J. Savage and I. Tolstoy. The scattered acoustic boundary wave generated by grazing at a slightly rough rigid surface. J. Acoust Soc Am 66 (4) 1131-1145 (1979).

6. W. A. Kinney, C. S. Clay and G. A. Sandness. Scattering from a corrugated surface: Comparison between experiment, Helmholtz-Kirchhoff theory, and the facet-ensemble method. J. Acoust Soc Am 73 (1) 183-194 (1983).

7. W. A. Kinney and C. S. Clay. The spacial coherence of sound scattered from a wind-driven surface. Comparison between experiment, Eckort theory, and the facet-ensemble method. J. Acoust Soc Am Vol 75 (1) 145-148 (1984).

8. H. Medwin. Specular scattering of underwater sound from a wind-driven surface. J. Acoust Soc Am Vol 41 (6) 1485-1495 (1967).

9. C. S. Clay, H. Medwin and W. M. Wright. Specularly scattered sound and the probability density function of a rough surface. J. Acoust Soc Am Vol 53 (6) 1677-1682 (1973).

10. S. K. Numrich and E. Callen. Scattering of acoustic waves from rough surfaces. Final Report. Naval Research Laboratory, Washington, DC Work Unit No. NR RR032-05-01 (1979).

11. C. Ecart. The scattering of sound from the sea surface. J. Acoust Soc Am 25 (3) 566-570 (1953).

12. C. W. Horton and T. G. Muir. Theoretical studies of the scattering of acoustic waves from a rough surface. J. Acoust Soc Am Vol 42 (3) 627-634 (1967).

13. M. L. Boyd and R. L. Deavonport. Forward and specular scattering from a rough surface: theory and experiment. J. Acoust Soc Am Vol 53 (3) 791-801 (1973).

14. C. W. Horton and D. R. Metton. Importance of the Fresnel correct in scattering from a rough surface. II. Scattering coefficient. J. Acoust Soc Am Vol 47 (1 pt 2) 290-303 (1970).

15. C. S. Clay and H. Medwin. Dependence of Spacial and temporal correlation of forward underwater sound on the surface statistics. I Theory Vol 47 (5 pt) 1412-1429 (1970).

16. A. K. Fung and A. Leovaris. Experimental verification of the proper Kirchhoff theory of wave scattering from known randomly rough surfaces. J. Acoust Soc Am Vol 46 (5 pt 1) 1057-1061 (1969).

17. P. J. Westervelt. Parametric acoustic array. J. Acoust Soc Amer 35 (4) 535-537 (1963).

18. R. T. Beyer. Nonlinear Acoustics. Published by U.S. Naval ships system command (1974).

19. H. O. Berktay. New directions in Physical Acoustics. LXIII Corso Soc. Italiana di Fiscica, Bolognal, Italy (1976).

20. Conference on Underwater applications of non-linear acoustics held at Uni Bath, England 10-11 Sept (1979).

21. M.B. Moffett and R. H. Mellen. Model for parametric acoustic sources. J. Acoust. Soc. Am. Vol 61 No 2 (1977).

22. R. J. Urick. Principles of underwater sound. McGraw-Hill, New York, (1975).

23. F. G. Bass and I. M. Fuks. Wave scattering from statistically rough surfaces. Pergamon Press, Oxford Chap 7 (1979).

24. C. S. Clay and H. Medwin. Acoustical oceanograph. John Wiley and Sons, Inc publication (1977).

25. P. D. Thorne and N. G. Pace. Acoustic studies of broadband scattering from a model rough surface. J. Acoust Soc Am 75 (1) 133-144 (1984).

26. N. G. Pace, Z. K. S. Al-Hamdani and P. D. Thorne. The range dependence of normal incidence acoustic backscatter from a rough surface. J. Acoust Soc Am 77 (1) 101-112 (1985).

27. D. F. McCammon and S. T. McDaniel. Surface reflection: On the convergence of a series solution to a modified Helmholtz integral equation and the validity of the Kirchhoff approximation. J. Acoust Soc Am 79 (1) 64-70 (1986).

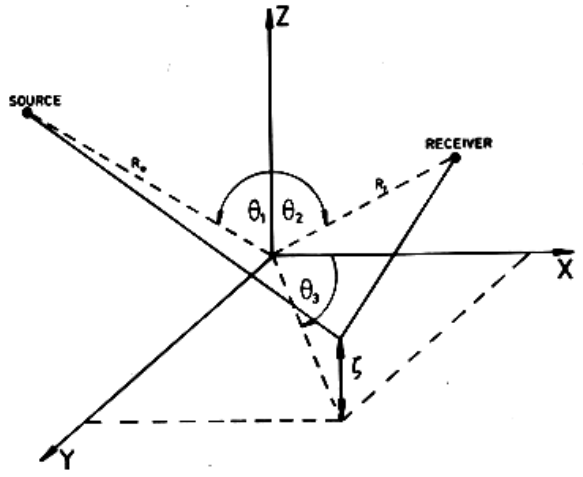

Fig. 1 Scattering geometry.

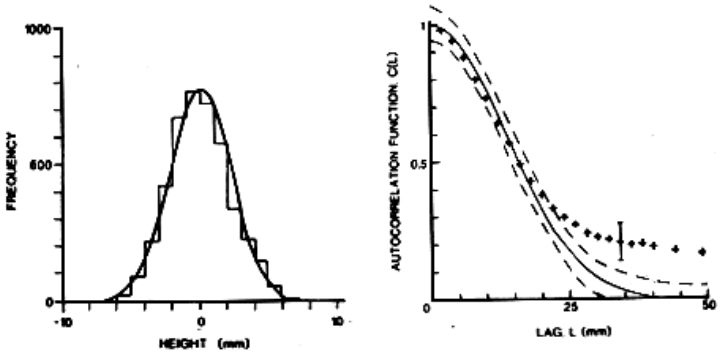

Fig. 2 Comparison of the statistics for the expanded polyurethane surface with gaussian statistics. —— gaussian curve.

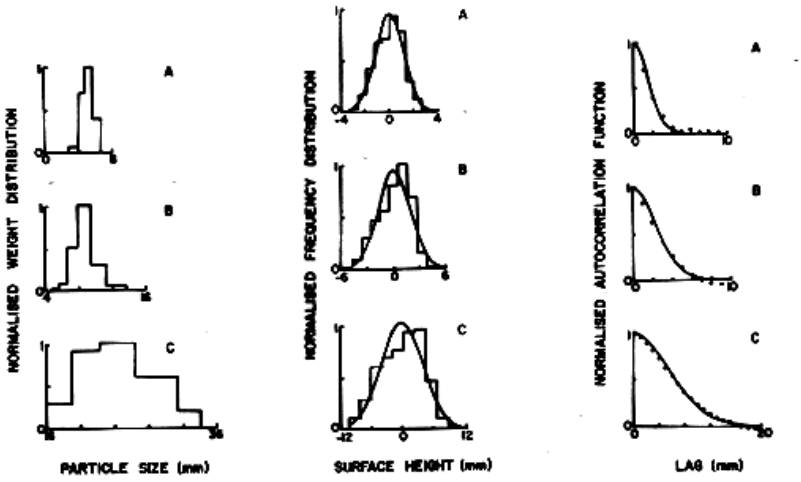

Fig. 3 Statistics of the three gravel surfaces. —— Comparison with a gaussian surface.

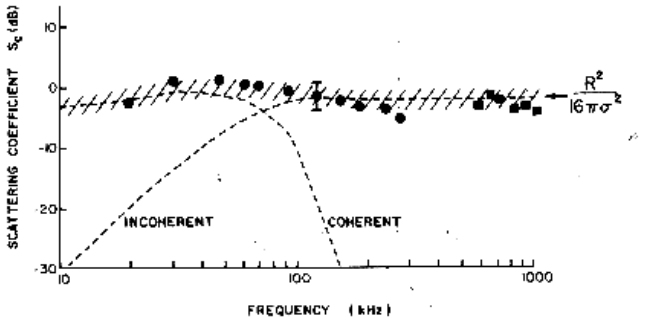

Fig. 4 Broadband normal incident backscattering from the expanded polyurethane surface. //// equation (5) with 1 s.d. allowance for errors in the measured parameters.

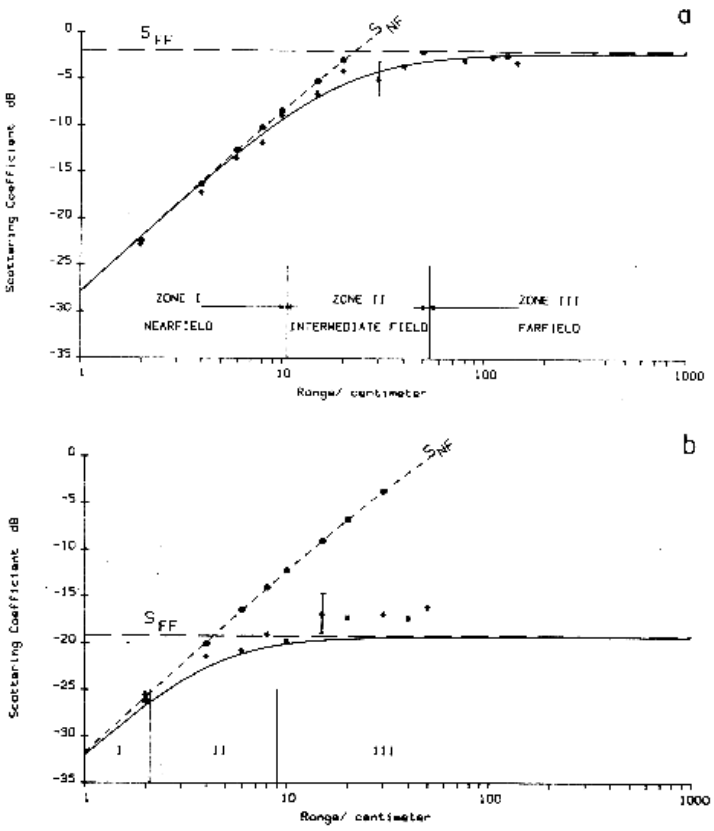

Fig. 5 Range dependence scattering from the expanded polyurethane surface (a) and (b) gravel surface B. —— equation (10), S_{FF}: equation (7), S_{NF}: equation (11), • Plane surface results. * Rough surface values.

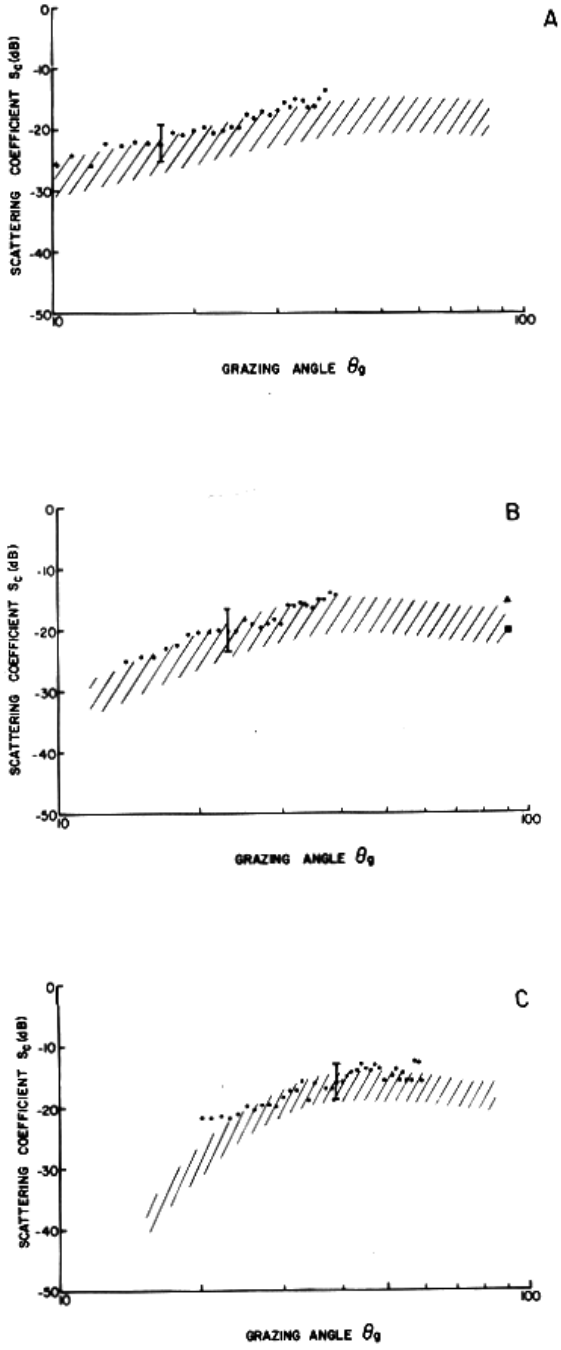

Fig.6 Backscattering from the three gravel surfaces. //// equation (12) with 1 s.d. allowance for the errors in the measured parameters.